Antiderivative Antialiasing for Memoryless Nonlinearities

Stefan Bilbao, Senior Member, IEEE, Fabián Esqueda, Graduate Student Member, IEEE, Julian D. Parker, and Vesa Välimäki, Fellow, IEEE

Abstract—Aliasing is a commonly-encountered problem in audio signal processing, particularly when memoryless nonlinearities are simulated in discrete time. A conventional remedy is to operate at an oversampled rate. A new aliasing reduction method is proposed here for discrete-time memoryless nonlinearities, which is suitable for operation at reduced oversampling rates. The method employs higher order antiderivatives of the nonlinear function used. The first order form of the new method is equivalent to a technique proposed recently by Parker et al. Higher order extensions offer considerable improvement over the first antiderivative method, in terms of the signal-to-noise ratio. The proposed methods can be implemented with fewer operations than oversampling and are applicable to discrete-time modeling of a wide range of nonlinear analog systems.

Index Terms—Aliasing, harmonic distortion, nonlinear systems, signal denoising, signal processing algorithms.

I. Introduction

ALIASING is a fundamental problem in nonlinear signal processing. When a digital signal undergoes a nonlinear operation, its bandwidth is expanded, leading to a spurious mirroring of components back to the baseband. Aliasing is particularly problematic in audio applications. This letter proposes an approach to aliasing suppression suitable for the simulation of memoryless nonlinearities in discrete time.

A commonly used method to reduce aliasing in memoryless nonlinearities is oversampling [1], [2], [3], [4], [5], [6], [7]. In audio applications, the input signal is typically upsampled by a factor of 8 or 16 using an appropriate interpolation filter. When the nonlinear function is applied at the oversampled rate, distortion components will appear at frequencies well above the original Nyquist limit. Under a downsampling/lowpassing operation, such components are suppressed, and aliasing will be negligible. The main disadvantage of oversampling is the proportional increase in the operation count. Interpolation/decimation filters add to the workload per sample.

Other approaches to antialiasing have been proposed for memoryless nonlinearities. Schattschneider and Zölzer [8] introduced a harmonic mixer model for polynomial nonlinearities of finite order. In the harmonic mixer, the nonlinearity is divided into a parallel structure in which each branch has a nonlinear function of a single order only and the branch input signals are lowpass filtered to assure that no aliasing can occur [8], [5]. A filterbank form was presented in [9]. Thornburg suggested that a nonlinear function could be approximated with a lower-order polynomial to reduce aliasing [1]. However, many useful nonlinear functions, such as the hard clipper [10], [2], [11], [12] and saturating functions [13], [14], [15], [16], [17], [18], cannot be approximated well with a polynomial. Recent work has applied bandlimited correction functions commonly used in oscillator synthesis to reduce the aliasing introduced by hard clipping and rectification [19], [20], [21].

Antialiasing methods of a fundamentally different character have been recently proposed by Parker et al. [22]. This method is based on approximating the underlying continuous-time input signal with a piecewise linear function, applying a nonlinear function to it, and convolving the resulting signal with the continuous-time impulse response of a lowpass filter.

In this letter, we present a new discrete-time aliasing reduction method for memoryless nonlinearities, based on discrete differentiation of higher order antiderivatives. The first-order method is equivalent to that in [22]. However, the use of higher antiderivatives leads to increasing levels of aliasing suppression; such methods are distinct from e.g. the second-order method presented in [22]. Such methods are applicable regardless of the particular form of the nonlinear function; aliasing suppression may be understood, intuitively, in terms of operation over increasingly smoothed forms of the nonlinearity. The proposed idea of differentiating antiderivatives is related to previous antialiasing synthesis methods called the differential polynomial waveform [23], [24], [25], [26], [27], and integrated wavetable/sampling synthesis [28], [29], [30].

This letter is organized as follows. Sec. II discusses the context of this work and the first-order antiderivative antialiasing method [22], which is the starting point for this work. Sec. III derives the new method using higher order antiderivates of the nonlinear function. Sec. IV evaluates the proposed method in terms of signal-to-noise ratio and compares it with the trivial, oversampled, and first-order methods using a hard-clipping and a hyperbolic tangent function as examples. Sec. V concludes this letter and lists ideas for further work.

II. Background

This letter deals with memoryless nonlinearities of the form

$$y(t) = F_0\left((x(t)\right). \tag{1}$$

Here, $x(t)$ is an input signal, and $y(t)$ is an output signal; both are assumed defined for $t \in \mathsf{R}$. F_0 is a real-valued mapping,

This work was supported by the European Research Council, under grant number ERC-2011-StG-279068-NESS, and the Aalto ELEC Doctoral School.

S. Bilbao is with the Acoustics and Audio Group, University of Edinburgh, Edinburgh EH9 3JZ, UK (e-mail: sbilbao@staffmail.ed.ac.uk).

F. Esqueda and V. Välimäki are with the Department of Signal Processing and Acoustics, Aalto University, FI-00076 AALTO, Espoo, Finland (e-mail: fabian.esqueda@aalto.fi; vesa.valimaki@aalto.fi).

J. D. Parker is with Native Instruments GmbH, Berlin, Germany (e-mail: julian.parker@native-instruments.com).

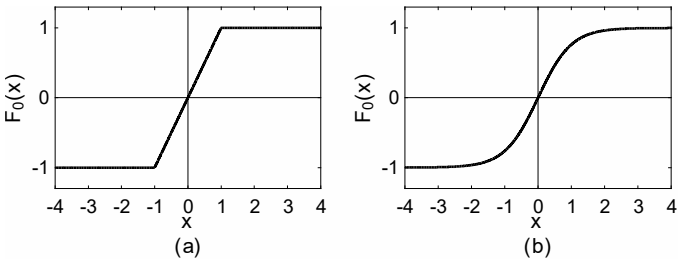

Fig. 1. Input–output relationships for (a) the hard clipper and (b) the hyperbolic tangent.

assumed continuous, but not necessarily differentiable, and in most cases of interest is nonlinear. Two typical examples of memoryless nonlinear mappings are the saturator, defined by

$$F_0(x) = \frac{1}{2}\left(|x+1| - |x-1|\right), \tag{2}$$

and the soft-clipping nonlinearity, defined by

$$F_0(x) = \tanh(x). \tag{3}$$

Fig. 1 shows the input–output relationships for these functions.

In the discrete setting, consider a real-valued input sequence x^{n}, for $n \in \mathsf{Z}$. Such a sequence could represent samples of the continuous function $x(t)$, for $t = nT$, where T is a sample period (and $f_{\mathsf{s}} = 1/T$ is the sample rate), or could be entirely synthetic. A direct approach to discrete-time emulation of (1) is to simply compute an output sequence y^{n} as

$$y^{\mathsf{n}} = F_0\left(x^{\mathsf{n}}\right). \tag{4}$$

As is well-known, such a trivial implementation generates aliased components, of strength depending on the smoothness of the mapping F_0, and the amplitude of the input signal x^{n} [1], [19], [20]. The usual approach to reducing aliasing is to operate at an oversampled rate, as discussed in Sec. I.

A. First-Order Antialiasing

In a recent paper, Parker **et al.** presented a novel algorithm for the reduction of aliasing in discrete-time memoryless nonlinearities, and suitable for operation at a non-oversampled rate [22]. It takes on a particularly simple form:

$$y^{\mathsf{n}} = \frac{F_1^{\mathsf{n}} - F_1^{\mathsf{n}-1}}{x^{\mathsf{n}} - x^{\mathsf{n}-1}}. \tag{5}$$

Here, $F_1^{\mathsf{n}} = F_1\left(x^{\mathsf{n}}\right)$ represents the first antiderivative of F_0 evaluated at x^{n}. The approximation (5) is arrived at after a number of steps. In particular, the input sequence x^{n} is assumed drawn from samples of a piecewise linear underlying function $x(t)$, which is then convolved with a box function of one sample duration, and then resampled. The convolution operation mentioned above requires the evaluation of the antiderivative of F_0, leading directly to the form in (5).

In the case of the saturator (2) and the soft-clip nonlinearity (3) the antiderivatives can be given, respectively, as

$$F_1(x) = \frac{1}{4}(x+1)^2\mathrm{sgn}(x+1) - (x-1)^2\mathrm{sgn}(x-1) - 2, \tag{6}$$

where $\mathrm{sgn}(\cdot)$ is the sign function, and

$$F_1(x) = \ln\left(\cosh(x)\right). \tag{7}$$

III. Higher-order Antiderivative Antialiasing

Though it is derived using signal processing considerations in [22], one observation that can be made about the antialiasing method (5) is that it represents an approximation to

$$y(x) = \frac{dF_1}{dx} \quad \text{or} \quad y(t) = \frac{dF_1/dt}{dx/dt}. \tag{8}$$

It is natural to examine extensions of the method (5), based on repeated antidifferentiation. In particular, consider the extension to pth order of (5):

$$y(x) = \frac{d^{\mathsf{p}}F_{\mathsf{p}}}{dx^{\mathsf{p}}} = D^{\mathsf{p}}F_{\mathsf{p}} \quad \text{where} \quad D = \frac{1}{dx/dt}\frac{d}{dt}, \tag{9}$$

where F_{p} is the pth antiderivative of F_0 to within a polynomial of degree $p-1$. It is important to point out that except in special cases, such as the saturator in (2), these are not available in closed form.

A. A Numerical Method

The key operation in (9) is repeated composition with the differential operator D. In order to construct a discrete-time approximation to the higher order forms in (9), it is useful to take an approach based on operator composition through discrete time approximations to D. For an arbitrary sequence g^{n}, $n \in \mathsf{Z}$, define unit forward and backward shifts e_+ and e_-, and associated first difference operations δ_+ and δ_- as

$$e_{\pm}g^{\mathsf{n}} = g^{\mathsf{n}\pm1} \quad \text{and} \quad \delta_{\pm} = \pm\left(e_{\pm} - 1\right). \tag{10}$$

Given an input sequence x^{n} and a sequence $q^{\mathsf{n}} = q(x^{\mathsf{n}})$, for some nonlinear mapping q, define the operators D_- and D_2, through their action on the time series q^{n} as

$$D_-q^{\mathsf{n}} = \frac{\delta_-q^{\mathsf{n}}}{\delta_-x^{\mathsf{n}}} \;\mathsf{u}\; Dq(x^{\mathsf{n}}) \tag{11}$$

$$D_2q^{\mathsf{n}} = \frac{2}{\left(e_+ - e_-\right)x^{\mathsf{n}}}\delta_+D_-q^{\mathsf{n}} \;\mathsf{u}\; D^2q(x^{\mathsf{n}}). \tag{12}$$

D_- is a one-sided approximation to D, and D_2 is a centered approximation to D^2.

Supposing that $p = 2m + r$, where $m = \mathsf{b}p/2\mathsf{c}$ and $r = \mathrm{mod}(p, 2)$, then a discrete-time approximation to (9) may be written, in operator form, as

$$y^{\mathsf{n}} = e_-^{\mathsf{m}}D_-^{\mathsf{r}}D_2^{\mathsf{m}}F_{\mathsf{p}}^{\mathsf{n}}, \tag{13}$$

where $F_{\mathsf{p}}^{\mathsf{n}} = F_{\mathsf{p}}\left(x^{\mathsf{n}}\right)$ and where the m sample unit delay e_-^{m} is used to render the approximation causal. When written explicitly to orders $p = 1, 2$, and 3, the approximation yields

$$y^{\mathsf{n}} = \frac{F_1^{\mathsf{n}} - F_1^{\mathsf{n}-1}}{x^{\mathsf{n}} - x^{\mathsf{n}-1}}, \tag{14}$$

$$y^{\mathsf{n}} = \frac{2}{x^{\mathsf{n}} - x^{\mathsf{n}-2}}\left(\frac{F_2^{\mathsf{n}} - F_2^{\mathsf{n}-1}}{x^{\mathsf{n}} - x^{\mathsf{n}-1}} - \frac{F_2^{\mathsf{n}-1} - F_2^{\mathsf{n}-2}}{x^{\mathsf{n}-1} - x^{\mathsf{n}-2}}\right), \tag{15}$$

and

$$y^{\mathsf{n}} = \frac{1}{x^{\mathsf{n}-1} - x^{\mathsf{n}-2}} \times \left[\frac{2}{x^{\mathsf{n}} - x^{\mathsf{n}-2}} \left(\frac{F_3^{\mathsf{n}} - F_3^{\mathsf{n}-1}}{x^{\mathsf{n}} - x^{\mathsf{n}-1}} - \frac{F_3^{\mathsf{n}-1} - F_3^{\mathsf{n}-2}}{x^{\mathsf{n}-1} - x^{\mathsf{n}-2}} \right) - \frac{2}{x^{\mathsf{n}-1} - x^{\mathsf{n}-3}} \left(\frac{F_3^{\mathsf{n}-1} - F_3^{\mathsf{n}-2}}{x^{\mathsf{n}-1} - x^{\mathsf{n}-2}} - \frac{F_3^{\mathsf{n}-2} - F_3^{\mathsf{n}-3}}{x^{\mathsf{n}-2} - x^{\mathsf{n}-3}} \right) \right]. \quad (16)$$

It can be seen that (14) is equivalent to (5), the method presented in [22]. However, (15) and (16) are its novel extensions. In practice, though aliasing is indeed suppressed, such methods do introduce a degree of linear filtering to the original signal, and thus all evaluation in Sec. IV will be carried out at a 2× oversampled rate.

B. Precision and Ill-Conditioning

The operations D_- and D_2 both include divisions by differences of signal values; there is thus the risk of loss of precision or division by zero when the denominator is small. Special approximations are necessary under such conditions.

The discrete-time approximation (13) consists of a sequence of operations of the form D_- or D_2. Consider a given function $G_0(x)$ and its first and second antiderivatives $G_1(x)$ and $G_2(x)$, as well as the sequences $G_0^{\mathsf{n}} = G_0(x^{\mathsf{n}})$, $G_1^{\mathsf{n}} = G_1(x^{\mathsf{n}})$, and $G_2^{\mathsf{n}} = G_2(x^{\mathsf{n}})$.

At time steps n for which $|x^{\mathsf{n}} - x^{\mathsf{n}-1}| \leq \epsilon$, for some threshold value ϵ, the following approximation to D_-, obtained through Taylor expansion, may be used:

$$D_- G_1^{\mathsf{n}} = G_0(\bar{x}^{\mathsf{n}-\frac{1}{2}}), \quad \bar{x}^{\mathsf{n}-\frac{1}{2}} = \frac{1}{2}\left(x^{\mathsf{n}} + x^{\mathsf{n}-1}\right). \quad (17)$$

This corresponds to the rule used in [22].

At time steps n for which $|x^{\mathsf{n}+1} - x^{\mathsf{n}-1}| \leq \epsilon$, for some threshold value ϵ, the following approximation to D_2 may be used:

$$D_2 G_2^{\mathsf{n}} = \frac{2}{\Delta}\left(G_1\left(\bar{x}^{\mathsf{n}}\right) + \frac{G_2^{\mathsf{n}} - G_2\left(\bar{x}^{\mathsf{n}}\right)}{\Delta}\right), \quad (18)$$

where

$$\bar{x}^{\mathsf{n}} = \frac{1}{2}\left(x^{\mathsf{n}+1} + x^{\mathsf{n}-1}\right), \quad \Delta^{\mathsf{n}} = \bar{x}^{\mathsf{n}} - x^{\mathsf{n}}. \quad (19)$$

When $|\Delta^{\mathsf{n}}| \leq \epsilon$, the further approximation

$$D_2 G_2^{\mathsf{n}} = G_0\left(\frac{1}{2}\left(\bar{x}^{\mathsf{n}} + x^{\mathsf{n}}\right)\right) \quad (20)$$

may be employed.

IV. Evaluation

The antialiasing characteristics of the proposed methods are easily observed in the case of a sinusoidal input. Fig. 2(a) shows the magnitude spectrum of a 1661-Hz sinewave (note G#6) with peak amplitude 10 under trivial hard clipping. A sample rate $f_\mathrm{s} = 44.1\,\mathrm{kHz}$ was used for this example. As a reference, Fig. 2(b) shows the spectrum of this signal upsampled by a factor of 6 prior to clipping. To bypass the effects of interpolation/decimation filters, the input signal was synthesized at the target rate $f_\mathrm{s} = 264.6\,\mathrm{kHz}$. The nonlinearity clearly introduces high levels of aliasing distortion throughout the spectrum which can be reduced using oversampling.

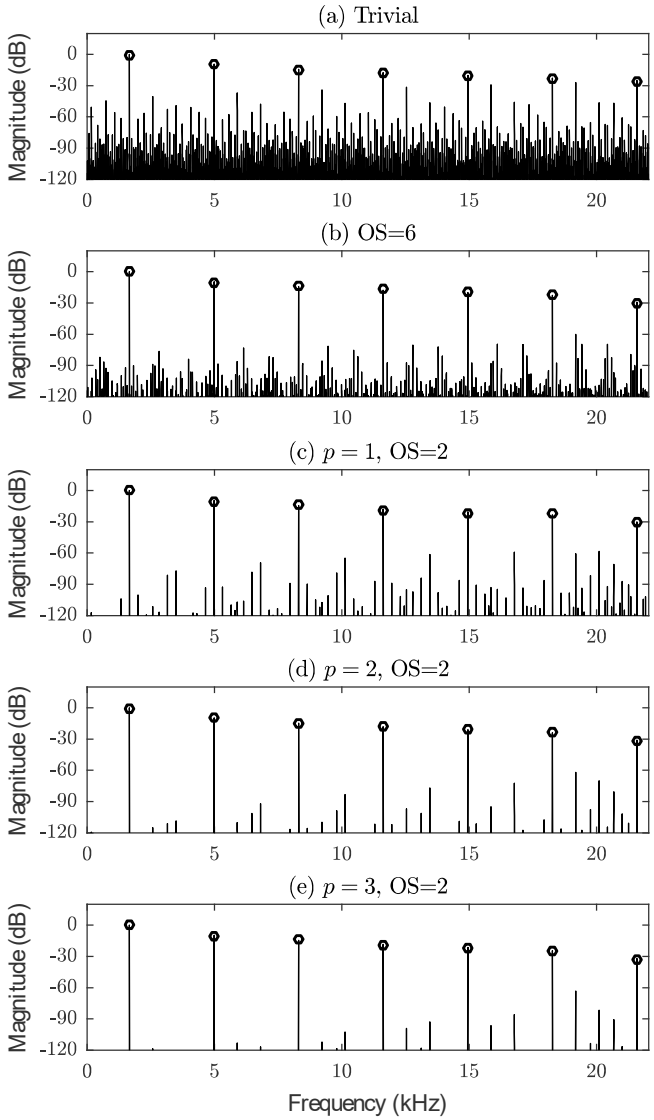

Fig. 2. Comparison of magnitude spectra for a 1661-Hz sinusoidal signal of amplitude 10 under hard clipping: (a) at a sample rate of 44.1 kHz, (b) when oversampled by a factor of 6, and when oversampled by a factor 2, and employing (c) the first-order antiderivative method and, (d)–(e) the proposed second-order and third-order antiderivative forms, respectively. The harmonic components are indicated with circles; all other spectral components are caused by aliasing.

Figs. 2(c)–(e) show the magnitude spectrum of the 1661-Hz sinewave processed using the first-order antiderivative method presented in [22] and the proposed extension (13) to second and third order. The methods were implemented using two-times oversampling, i.e. $f_\mathrm{s} = 88.2\,\mathrm{kHz}$. In particular, aliasing is suppressed more at low frequencies, which is advantageous in audio, because at frequencies below the first harmonic, the audibility of disturbances is limited only by the hearing threshold whereas auditory masking makes high-frequency disturbances between harmonics inaudible [31].

The performance of the proposed methods was evaluated by measuring the signal-to-noise ratio (SNR) for a set of

TABLE I
AVERAGED PROCESSING TIMES (PER SECOND) FOR OVERSAMPLING BY 6 AND THE ANTIDERIVATIVE FORMS

Nonlinearity	OS = 6	$p = 1$	$p = 2$	$p = 3$
Hard Clipping	0.23 s	0.10 s	0.15 s	0.17 s
Hyperbolic Tangent	0.46 s	0.19 s	0.21 s	0.23 s

sinusoidal inputs. The SNR was defined as the power ratio between the desired part of the signal, and the components generated by aliasing, or residual. Following [23], an ideal alias-free version of each test signal was synthesized using Fourier analysis and additive synthesis. This bandlimited signal was subtracted from the aliased signal to yield the residual. Since in audio applications the SNR is only meaningful at audible frequencies, all signals were lowpass filtered to 16 kHz prior to the SNR evaluation. As before, algorithms (14)–(16) were implemented using an oversampling factor of 2 (i.e. $f_s = 88.2$ kHz). Given the high computational costs of evaluating the hyperbolic tangent function and its antiderivatives at every time step, a lookup table (LUT) was employed using cubic Lagrange interpolation. Each LUT was generated by evaluating each nonlinearity at a thousand points between 0 and 10, and employing odd symmetry. Interpolation error relative to analytical values was in the range of 10^{-15}.

Figs. 3(a) and (b) show the SNRs for sinusoidal signals with fundamental frequencies between 1 and 10 kHz under hard clipping (2) and soft saturation (3), respectively. As a reference, trivial audio rate processing and oversampling by factor 6 are also shown. For hard clipping, the second- and third-order forms increase SNR by approx. 15 and 30 dB w.r.t. oversampling by factor 6 [cf. Fig. 3(a)]. In the case of the soft-clipper [cf. Fig. 3(b)], the third-order method outperforms oversampling by 6 for high fundamental frequencies. At lower fundamentals the SNRs lie above 96 dB, which can already be considered sufficient for 16-bit audio (CD quality) [32].

The third-order form requires one nonlinear function evaluation, one multiplication, one addition and two divisions per output sample. The remaining calculations correspond to previous evaluations and can be stored in memory. For comparison, the four methods discussed here were run in Python on an Apple iMac with an Intel Core i5 (2.7 GHz) processor with 16 GB of 1600 MHz DDR3 RAM. A 10-second linear sine sweep from 1–10 kHz with input gain 10 was used as an input signal. As before, the hyperbolic tangent and its antiderivatives were implemented using LUTs. Table I compares the average computation times per second for oversampling by factor 6 and the antiderivative forms. These results demonstrate that the proposed methods are more efficient than oversampling. In practice the additional cost of interpolation/decimation filters required for oversampling must also be taken into account, constituting a further advantage of the antiderivative methods.

V. CONCLUSION AND FURTHER WORK

A new approach to antialiasing for discrete-time nonlinearities has been presented here. It is of a general character,

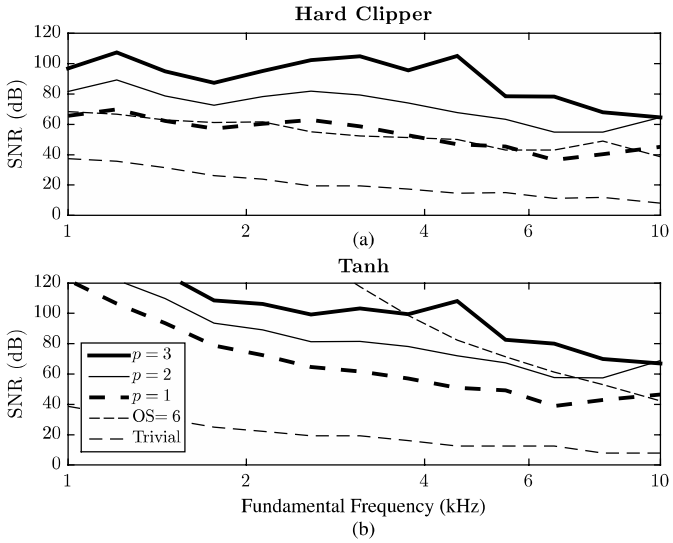

Fig. 3. SNR of sinewaves under (a) hard and (b) soft clipping implemented trivially ($f_s = 44.1$ kHz), oversampled by 6 (OS = 6), employing oversampling by factor 2 and, the first-order method ($p = 1$) and the proposed antiderivative forms ($p = 2$, 3).

more efficient than oversampling, and does not depend on the particular type of nonlinearity, or on a simplification of its functional form. It is presented here as a family of methods of increasing order p of antidifferentiation in the nonlinearity, leading, ultimately, to an increasing degree of aliasing suppression. As is natural, computational cost also scales with the order p. There remain many open questions and avenues of future research.

A series of discrete approximations to (9) is given in (13) which a) maintain the nested structure of the underlying equation, and b) for a given order p, are minimal in terms of the number of signal values used to compute an approximation, which is $p + 1$. An inherent characteristic of this family of methods is that of spectral shaping of the output; though aliasing is suppressed, there can be some attenuation of the signal in the high frequency range. Additional linear filtering is one option in this case, as suggested in [33], [34] for antialiased oscillators. Given that neither property a) nor b) is necessary in the approximation of (9), generalisations beyond the nested structures presented here could aid in finding antialiasing methods for which such attenuation is reduced.

Only the single memoryless nonlinearity has been discussed here. A logical extension will be to multiple such nonlinearities in a feedback setting, as it is currently one of the main applications of virtual analog modeling in audio [35], [36], [37], [38], [12]. A major new consideration will be the determination of numerical stability conditions for such antialiasing methods, and will form the basis for future investigations.

VI. ACKNOWLEDGMENT

The main part of this work was conducted in June 2016, during a visit by F. Esqueda, J. D. Parker, and V. Välimäki to the University of Edinburgh.

REFERENCES

[1] H. Thornburg, "Antialiasing for nonlinearities: Acoustic modeling and synthesis applications," in *Proc. Int. Comput. Music Conf.*, Beijing, China, Oct. 1999, pp. 66–69.

[2] P. Kraght, "Aliasing in digital clippers and compressors," *J. Audio Eng. Soc.*, vol. 48, no. 11, pp. 1060–1064, Nov. 2000.

[3] J. Pakarinen and M. Karjalainen, "Enhanced wave digital triode model for real-time tube amplifier emulation," *IEEE Trans. Audio Speech Lang. Process.*, vol. 18, no. 4, pp. 738–746, May 2010.

[4] F. Fontana and M. Civolani, "Modeling of the EMS VCS3 voltage-controlled filter as a nonlinear filter network," *IEEE Trans. Audio Speech Lang. Process.*, vol. 18, no. 4, pp. 760–772, May 2010.

[5] P. Dutilleux, K. Dempwolf, M. Holters, and U. Zölzer, "Nonlinear processing," in *DAFX: Digital Audio Effects*, U. Zölzer, Ed. Chichester, UK: Wiley, 2011, pp. 101–138.

[6] F. Eichas, S. Möller, and U. Zölzer, "Block-oriented modeling of distortion audio effects using iterative minimization," in *Proc. Int. Conf. Digital Audio Effects (DAFx-15)*, Trondheim, Norway, Sept. 2015, pp. 243–248.

[7] D. Hernandez and J. Huang, "Emulation of junction field-effect transistors for real-time audio applications," *IEICE Electronics Express*, vol. 13, no. 12, June 2016.

[8] J. Schattschneider and U. Zölzer, "Discrete-time models for nonlinear audio systems," in *Proc. Digital Audio Effects Workshop*, Trondheim, Norway, Dec. 1999, pp. 45–48.

[9] P. Fernández-Cid and J. Casajús-Quirós, "Distortion of musical signals by means of multiband waveshaping," *J. New Music Research*, vol. 30, no. 3, pp. 279–287, 2001.

[10] D. Rossum, "Making digital filters sounds analog," in *Proc. Int. Computer Music Conf.*, San Jose, CA, Oct. 1992, pp. 30–33.

[11] F. Santagata, A. Sarti, and S. Tubaro, "Non-linear digital implementation of a parametric analog tube ground cathode amplifier," in *Proc. Int. Conf. Digital Audio Effects (DAFx-07)*, Bordeaux, France, Sept. 2007, pp. 169–172.

[12] A. Falaize and T. Hélie, "Passive guaranteed simulation of analog audio circuits: A port-Hamiltonian approach," *Appl. Sci.*, vol. 6, no. 10, p. 273, May 2016.

[13] A. Huovilainen, "Non-linear digital implementation of the Moog ladder filter," in *Proc. Int. Conf. Digital Audio Effects (DAFx-04)*, Naples, Italy, Oct. 2004, pp. 61–164.

[14] J. Pakarinen and D. T. Yeh, "A review of digital techniques for modeling vacuum-tube guitar amplifiers," *Computer Music J.*, vol. 33, no. 2, pp. 85–100, 2009.

[15] T. Hélie, "Volterra series and state transformation for real-time simulations of audio circuits including saturations: Application to the Moog ladder filter," *IEEE Trans. Audio Speech Lang. Process.*, vol. 18, no. 4, pp. 747–759, May 2010.

[16] D. T. Yeh, J. S. Abel, and J. O. Smith, "Automated physical modeling of nonlinear audio circuits for real-time audio effects—Part I: Theoretical development," *IEEE Trans. Audio Speech Lang. Process.*, vol. 18, no. 4, pp. 728–737, May 2010.

[17] R. C. D. de Paiva, J. Pakarinen, V. Välimäki, and M. Tikander, "Real-time audio transformer emulation for virtual tube amplifiers," *EURASIP J. Adv. Signal Process*, vol. 2011, pp. 1–15, Feb. 2011.

[18] S. D'Angelo, J. Pakarinen, and V. Välimäki, "New family of wave-digital triode models," *IEEE Trans. Audio Speech Lang. Process.*, vol. 21, no. 2, pp. 313–321, Feb. 2013.

[19] F. Esqueda, V. Välimäki, and S. Bilbao, "Aliasing reduction in soft-clipping algorithms," in *Proc. European Signal Processing Conf. (EUSIPCO 2015)*, Nice, France, Aug. 2015, pp. 2059–2063.

[20] F. Esqueda, S. Bilbao, and V. Välimäki, "Aliasing reduction in clipped signals," *IEEE Trans. Signal Process.*, vol. 60, no. 20, pp. 5255–5267, Oct. 2016.

[21] F. Esqueda, V. Välimäki, and S. Bilbao, "Rounding corners with BLAMP," in *Proc. Int. Conf. Digital Audio Effects (DAFx-16)*, Brno, Czech Republic, Sept. 2016, pp. 121–128.

[22] J. D. Parker, V. Zavalishin, and E. Le Bivic, "Reducing the aliasing of nonlinear waveshaping using continuous-time convolution," in *Proc. Int. Conf. Digital Audio Effects (DAFx-16)*, Brno, Czech Republic, Sept. 2016, pp. 137–144.

[23] V. Välimäki, "Discrete-time synthesis of the sawtooth waveform with reduced aliasing," *IEEE Signal Process. Lett.*, vol. 12, no. 3, pp. 214–217, Mar. 2005.

[24] V. Välimäki and A. Huovilainen, "Oscillator and filter algorithms for virtual analog synthesis," *Computer Music J.*, vol. 30, no. 2, pp. 19–31, 2006.

[25] V. Välimäki, J. Nam, J. O. Smith, and J. S. Abel, "Alias-suppressed oscillators based on differentiated polynomial waveforms," *IEEE Trans. Audio Speech Lang. Process.*, vol. 18, no. 4, pp. 786–798, May 2010.

[26] J. Kleimola and V. Välimäki, "Reducing aliasing from synthetic audio signals using polynomial transition regions," *IEEE Signal Process. Lett.*, vol. 19, no. 2, pp. 67–70, Feb. 2012.

[27] D. Ambrits and B. Bank, "Improved polynomial transition regions algorithm for alias-suppressed signal synthesis," in *Proc. 10th Sound and Music Computing Conf. (SMC2013)*, Stockholm, Sweden, Aug. 2013, pp. 561–568.

[28] G. Geiger, "Table lookup oscillators using generic integrated wavetables," in *Proc. Int. Conf. Digital Audio Effects (DAFx-06)*, Montreal, QC, Canada, Sept. 2006, pp. 169–172.

[29] A. Franck and V. Välimäki, "An ideal integrator for higher-order integrated wavetable synthesis," in *Proc. IEEE Int. Conf. Acoust. Speech Signal Process. (ICASSP-13)*, Vancouver, BC, Canada, May 2013, pp. 41–45.

[30] ——, "Higher-order integrated wavetable and sampling synthesis," *J. Audio Eng. Soc.*, vol. 61, no. 9, pp. 624–636, Sept. 2013.

[31] H.-M. Lehtonen, J. Pekonen, and V. Välimäki, "Audibility of aliasing distortion in sawtooth signals and its implications for oscillator algorithm design," *J. Acoust. Soc. Am.*, vol. 132, no. 4, pp. 2721–2733, Oct. 2012.

[32] U. Zölzer, "Introduction," in *Digital Audio Signal Processing*. Chichester, UK: Wiley, 2008, pp. 1–19.

[33] J. Pekonen, J. Nam, J. O. Smith, J. S. Abel, and V. Välimäki, "On minimizing the look-up table size in quasi-bandlimited classical waveform oscillators," in *Proc. Int. Conf. Digital Audio Effects (DAFx-10)*, Graz, Austria, Sept. 2010, pp. 419–422.

[34] V. Välimäki, J. Pekonen, and J. Nam, "Perceptually informed synthesis of bandlimited classical waveforms using integrated polynomial interpolation," *J. Acoust. Soc. Am.*, vol. 131, no. 1, pp. 974–986, Jan. 2012.

[35] S. D'Angelo and V. Välimäki, "Generalized Moog ladder filter: Part II—Explicit nonlinear model through a novel delay-free loop implementation method," *IEEE/ACM Trans. Audio Speech Lang. Process.*, vol. 22, no. 12, pp. 1873–1883, Dec. 2014.

[36] K. J. Werner, V. Nangia, J. O. Smith, and J. S. Abel, "A general and explicit formulation for wave digital filters with multiple/multiport nonlinearities and complicated topologies," in *Proc. IEEE Workshop Appl. Signal Process. Audio Acoust. (WASPAA-15)*, Oct. 2015, pp. 1–5.

[37] D. Medine, "Dynamical systems for audio synthesis: Embracing nonlinearities and delay-free loops," *Appl. Sci.*, vol. 6, no. 5, p. 134, May 2016.

[38] A. Bernardini, K. J. Werner, A. Sarti, and J. O. Smith III, "Modeling nonlinear wave digital elements using the Lambert function," *IEEE Trans. Circ. Syst. I: Regular Papers*, vol. 63, no. 8, pp. 1231–1242, Aug. 2016.